Journal of Power Sources 195 (2010) 1246–1255

Contents lists available at ScienceDirect

Journal of Power Sources

journal homepage: www.elsevier.com/locate/jpowsour

A polymer gel electrolyte composed of a poly(ethylene oxide) copolymer and the influence of its composition on the dynamics and performance of dye-sensitized solar cells

João E. Benedetti[a], Agnaldo D. Gonçalves[a], André L.B. Formiga[a], Marco-A. De Paoli[a], X. Li[b], James R. Durrant[b], Ana F. Nogueira[a,*]

[a] Institute of Chemistry, University of Campinas – UNICAMP, P.O. Box 6154, 13083-970 Campinas, SP, Brazil
[b] Centre for Electronic Materials and Devices, Imperial College of Science Technology and Medicine, London SW7 2AY, United Kingdom

ARTICLE INFO

Article history:
Received 6 August 2009
Received in revised form 2 September 2009
Accepted 2 September 2009
Available online 11 September 2009

Keywords:
Gel polymer electrolyte
Dye sensitized solar cells
Polyiodide formation
Transient absorption spectroscopy

ABSTRACT

A polymer gel electrolyte composed of a poly(ethylene oxide) derivative, poly(ethylene oxide-co-2-(2-methoxyethoxy) ethyl glycidyl ether), mixed with gamma-butyrolactone (GBL), LiI and I_2 is employed in dye sensitized solar cells (DSSC). The electrolyte is characterized by conductivity experiments, Raman spectroscopy and thermal analysis. The influence of the electrolyte composition on the kinetics of DSSC is also investigated by transient absorption spectroscopy (TAS). The electrolyte containing 70 wt.% of GBL and 20 wt.% of LiI presents the highest conductivity (1.9×10^{-3} S cm^{-1}). An efficiency of 4.4% is achieved using this composition. The increase in I_{SC} as a function of GBL can be attributed an increase in the mobility of the iodide (polyiodide) species. The increase in the yield of the intermediate species, I_2^-, originating in the regeneration reaction, is confirmed by TAS. However, the charge recombination process is faster at this composition and a decrease in the V_{oc} is observed. Photovoltage decay experiments confirm an acceleration in charge recombination for the DSSC assembled with the electrolyte containing more GBL. Raman investigations show that in this electrolyte the I_5^-/I_3^- ratio is higher. Theoretical calculations also indicate that the I_5^- species is a better electron acceptor.

1. Introduction

Dye-sensitized solar cells (DSSC) have attracted much attention since the pioneering work reported by O'Regan and Grätzel [1], especially in light of their potential low cost compared to conventional silicon-based solar cells. DSSC based on TiO_2 as the nanostructured electrode are capable of achieving efficiencies of 11% [2]. However, the presence of a liquid electrolyte demands a perfect seal in order to avoid leakage and evaporation of the solvent. Nonetheless, such perfect seals are difficult to obtain and usually the use of a liquid component results in poor long-term stability and performance of the entire device. Many efforts have been investigated to overcome this drawback, replacing the liquid electrolyte by room temperature ionic liquids [3,4] organic and inorganic hole transport materials [5–7], polymer and gel electrolytes [8–12].

Polymer electrolytes are usually exemplified by polyethers, such as poly(ethyelene oxide) (PEO) or poly(propylene oxide) (PPO) coordinated with a range of inorganic salts, such as LiI, NaI, $LiClO_4$, $LiCF_3SO_3$, LiSCN, NaSCN, $NaClO_4$ and $LiPF_6$ [13]. The solid nature of this material is a great advantage; however, the ionic conductivity which occurs in the amorphous phase for the majority of the polymer electrolytes is too low (10^{-8} to 10^{-5} S cm^{-1}), limiting the efficiency of devices, such as photoelectrochemical cells, batteries or electrochemical capacitors.

The mixture of a third component into the polymer/salt system can be used to increase the overall conductivity. One type of electrolyte is a "gel electrolyte", where small molecules or oligomers with high boiling points are added to the system [14]. When such additives are able to change the glass transition temperature of the pure polymer and, as a consequence increase the flexibility of the polymer chains, they are called plasticizers. In some cases, the plasticizers can also decrease the crystallinity phase of the polymer host. However, in most studies, these low molar mass additives added to a polymer electrolyte do not behave as a "real" plasticizer, but act as a solvent for both salt and polymer. These electrolytes are not true polymer electrolytes, as defined before, as their ionic transport resembles that of a liquid system and the polymer serves primarily as a support for the conducting matrix and also contributes to the dissociation of the salt. In classical gel electrolytes, polyacrylonitrile, poly(methyl methacrylate) or poly(vinylidene fluoride) derivatives are examples of inactive polymers that in a three-dimensional network can be exploited as a

* Corresponding author. Tel.: +55 19 3521 3029; fax: +55 19 3521 3023.
E-mail address: anaflavia@iqm.unicamp.br (A.F. Nogueira).

0378-7753/$ – see front matter © 2009 Elsevier B.V. All rights reserved.
doi:10.1016/j.jpowsour.2009.09.008

support for a electrolyte solution [15]. Gel electrolytes based on a polymer host such as PEO are also common and lots of examples can be found in literature [16]. Gel electrolytes provide ionic conductivities close to 1 mS cm^{-1}, however, the mechanical properties are poor. One alternative is to add (nano)fillers to the gel electrolyte to promote mechanical stability [11,17–19].

As there is a fuzzy separation between these terminologies, we think that it is important to address the difference between those types of polymer electrolytes, since this topic creates certain misinterpretations in the literature.

DSSC using polymer gel electrolytes present a better performance when compared to the same device assembled with a classical polymer electrolyte [20–22]. However, the overall conversion efficiency is still low in comparison to DSSC using liquid electrolytes. The major problems arise from the low ionic diffusion in a more viscous medium, limiting the photocurrent, the low penetration of polymer inside the nanostructured electrode, and an increase in the interfacial charge-transfer resistance between the electrodes and the electrolyte [23]. In order to enhance the overall conversion efficiency and, as a consequence, the transport properties, the nature of the polymer (gel) systems must be modified. Addition of inorganic nanofillers [19,18], crown ether molecules [24], ionic liquids [25–27], oligomers based on ethylene oxide [28,29], gelators [30,31], and compounds such as (*t*-butylpyridine, *t*-bromomethylbenzene, acetic acid and *gamma*-butyrolactone (GBL)) [32,33] have become a common route to elaborate polymer (or gel) electrolytes with improved ionic conductivity properties. Recently, we demonstrated how the LiI concentration in the copolymer poly(ethylene oxide-co-epichlorohydrin) affects the DSSC kinetics and its correlation with the device's efficiency [34]. In this previous study we varied the amount of LiI, keeping the GBL:polymer ratio constant at 50:50 and we monitored the regeneration/recombination reactions. The increase in the concentration of LiI and I_2 accelerates dye cation regeneration as measured by transient absorption spectroscopy (TAS); however, it also contributes to increase the dark current of the cell by an order of magnitude. The efficiency of solar cells employing the best electrolyte was 3.5% at 100 mW cm^{-2}. In this work, we present the full characterization (by Raman, thermal analysis and conductivity experiments) of a new polymer electrolyte based on poly (ethylene oxide-co-2-(2-methoxyethoxy)ethyl glycidylether) with different contents of GBL. The effect of GBL content on the kinetics and on the device's performance was also evaluated by TAS.

2. Experimental

2.1. Preparation of the polymer/gel electrolytes

Poly(ethylene oxide-co-2-(2-methoxyethoxy) ethyl glycidyl ether) P(EO-EM) was used as received from Daiso Co., Ltd. (Osaka, Japan). The ethylene oxide:2-(2-methoxyethoxy)ethyl glycidyl ether ratio in the copolymer was 78:22 and its molar mass was *ca.* 1×10^6 g mol^{-1}, according to the supplier. The polymer samples were prepared by the dissolution of the copolymer, LiI, I_2, gamma-butyrolactone (GBL) (Aldrich, 99%) in 15 mL of acetone. Each component was dissolved separately in acetone before mixing. The P(EO-EM):GBL ratios were 0.3:0.7, 0.5:0.5, and 0.7:0.3 (wt.%). Electrolyte solutions were kept under stirring for 1 week before use.

2.2. Ionic conductivity measurements

Ionic conductivity measurements were evaluated as a function of salt content for the gel polymer electrolytes prepared with different contents of GBL. All samples comprised a polymer electrolyte (film thickness ~100 μm) deposited by casting part of the electrolyte solution onto a Teflon disk, under saturated atmospheric conditions. Afterwards, the films were detached from the Teflon disk by dipping into liquid nitrogen, and further dried under controlled vacuum for at least 144 h. Conductivity measurements were carried out in an MBraun dry box (humidity <10^{-4}%, under an argon atmosphere). The films were fixed between two mirror-polished stainless steel disc-shaped electrodes (diameter = 12 mm) using a Teflon spacer (0.05 mm) to prevent short-circuits and to maintain a fixed thickness. The conductivity values were calculated from electrochemical impedance spectroscopy (EIS) data, using an Eco-Chemie PGSTAT 12, Autolab, Kanaalweg (Holland) with FRA module coupled to a computer, in the frequency range of 10^5 to 10 Hz and AC amplitude of 10 mV. The ionic conductivity values were calculated from the bulk electrolyte resistance values arising from the complex impedance diagram.

2.3. Raman spectroscopy

The Raman spectra of the gel polymer electrolyte samples were measured in a Raman spectrometer, Micro-Raman Renishaw System 3000, Renishaw Scientific, New Mills (United Kingdom), equipped with a CCD (charge coupled device) detector and an Olympus BTH 2 microscope. The excitation laser was set at 632.8 nm.

2.4. Thermal characterization of the polymer electrolytes

Differential scanning calorimetry (DSC) curves of the gel polymer electrolytes were measured on a T.A. Instruments model 2100 coupled to a T.A. 2100 data analysis system, T.A. instruments Twin Lakes (United States). Average sample weight was within the range of 18–20 mg. All experiments were performed under a nitrogen flow of 100 mL min^{-1}. The samples were first heated at 100 °C for 5 min to eliminate the thermal history. After cooling the samples to −100 °C at a rate of 10 °C min^{-1}, they were heated again to 100 °C at a rate of 10 °C min^{-1}. The DSC curves presented here are related to this second heating step.

2.5. Solar cell assembly and characterization

Solar cells were assembled with 0.25 cm^2 of active area. A TiO_2 suspension (Solaronix) was deposited by the doctor blading technique onto the TCO substrate (Hartford Glass Co., Inc., 8–12 Ω cm^{-2}). The films were heated to 450 °C for 30 min, giving a layer of ~8 μm thickness as measured with a Tencor Alpha-step 200 profilometer. The electrodes were immersed in a 1.5×10^{-4} mol L^{-1} solution of the complex [*cis-bis*(isothiocyanate) *bis*(2,2-bipyridyl-4,4-dicarboxylate]ruthenium(II) *bis*-tetrabutylammonium (also known as N-719, Solaronix) in anhydrous ethanol for 20 h at room temperature. Afterwards, the electrodes were washed with ethanol and dried in air. The polymer electrolyte deposition onto the TiO_2/dye films was done inside a vacuum chamber using the method introduced for Caruso and co-workers [35]. Vacuum helps to ensure a better penetration of the polymer electrolyte inside the pores. After, the substrates were placed onto a hot plate at 60 °C to remove acetone. The Pt counter electrodes were then pressed onto the top of the gel polymer electrolyte films.

J–V curves in the dark and under illumination (10 and 100 mW cm^{-2}) were obtained at standard AM 1.5 conditions using a Xe (Hg) lamp as light source and filters. The polychromatic light intensity at the electrode position was measured with a Newport Optical Power Meter model 1830-C. The *J–V* curves were fitted using a two diode equation [36]. The diode ideality factor m_1 and series resistance R_s values were estimated initially from the *J–V* curve in the dark. Then the m_2 and k (fitting constant) were calculated from the *J–V* curve under 100 mW cm^{-2} [36]. The voltage

decay measurements were carried out under open-circuit conditions by switching off the light and monitoring the open-circuit voltage (V_{oc}) decay in the dark for a given period of time [37,38]. The IPCE spectra of the 1.0 cm^2 solar cells were measured using a monochromator (Oriel) coupled to the optical bench described above.

Nanosecond to millisecond transient absorption data were conducted on the completed dye-sensitized solar cells assembled with the polymer electrolyte samples using home-built equipment; Imperial College (London). For the measurement of the transient absorption data, samples were excited at 530 nm employing a PTIGL-3300 pumped dye nitrogen laser (~0.1 mJ cm^{-2}, repetition rate 0.1–0.2 Hz, <1 ns duration). The probe light source was a 150 W tungsten lamp. The monitoring wavelength from the lamp was selected by using a monochromator, typically set to monitor the transient signal at 810 nm, which primarily results from dye cation absorption [39]. Appropriate monochromators and/or filters were used to minimize the probe light incident upon the sample. Transient data were collected with a silicon photodiode and digitized using a Tektronix TDS220 digital storage oscilloscope. The time resolution of the apparatus was ~300 ns. The data were collected under open-circuit and dark conditions. The current drawn by the cell was monitored during the whole experiment.

2.6. Theoretical calculations

Electron affinities were calculated using DFT and two different all-electron basis sets. To reproduce the work of Sharp and Gellene [40], equilibrium geometries for both monoanionic ions (I_3^- and I_5^-) were optimized using the SV4(2d) basis set under DFT with the hybrid B3PW91 method [41] and a restricted wave function.

Assuming these geometries, single point calculations were performed with two basis sets using an unrestricted wave function for all species. Calculated electron affinities were obtained as the energy differences between the dianionic and the monoanionic species.

The SV4(2d) basis [42] is a split-valence contraction [6s5p2d] of a primitive set (16s15p7d) and augmented with two d functions. The ANODZP basis is a polarized double-ζ contraction [6s5p3d1f] of a relativistic primitive set (22s19p13d5f3g) for iodine obtained by Roos et al. [43] based on CASSCF/CASPT2 using the Douglas–Kroll Hamiltonian.

Converged geometries reveal that symmetric linear I_3^- and bent I_5^- anions were obtained and accurately reproduce the previous work of Sharp and Gellene. Electron affinities were calculated considering the following gas-phase reaction in which x can be 3 or 5.

$$I_x^-(g) + 1e^- \rightarrow I_x^{2-}(g) E = -EA$$

Calculated electron affinities are negative quantities, which means that the attachment of one electron to the monoanionic species is an endothermic process.

3. Results and discussion

3.1. Ionic conductivity measurements

Fig. 1 shows the Nyquist and Bode plots for the gel electrolyte with different salt concentration and GBL contents, respectively. The Nyquist plots of the gel polymer electrolytes sandwiched between the two blocking electrodes did not exhibit the typical semicircle at the high frequency region (see the magnification region in Nyquist plots), normally observed when measuring the impedance of a classical polymer electrolyte (polymer and salt only) [44].

The disappearance of the semicircle in Nyquist plots is a consequence of the high conductivity of the samples, and a straight line was observed instead. The intersection of this line with the real axis, Z', provides the resistance value (R), which was used to calculate the ionic conductivity of the polymer electrolyte samples, according to equation [45–47]: $\sigma = l/AR_b$, where: (σ) is the ionic conductivity, (l) is the film thickness, (A) is the electrode area and (R) is the electrolyte resistance obtained from the intercept of the Nyquist plot with the real axis.

After calculations, Fig. 2 shows the ionic conductivity values for the electrolytes containing 30 wt.%, 50 wt.%, and 70 wt.% of GBL as a function of the LiI concentration. The iodide:iodine ratio was 10:1 (wt.%) for all samples. The inset in Fig. 2 shows a picture of the gel electrolyte with 20 wt.% LiI. No fluidity is observed at room temperature even after addition of 70 wt.% of GBL. This is an important feature for application as an electrolyte in DSSC.

Increasing the amount of GBL, an overall increase in conductivity is observed, reaching 1.9×10^{-3} S cm^{-1} for the sample containing 20 wt.% of LiI and 70 wt.% of GBL. This value is normally found in the literature for gel polymer electrolyte samples [16]. As will be discussed in the next section, the role of the GBL, the additive used here to improve ionic conductivity, is not as a plasticizer; instead, GBL acts as a solvent for both polymer and salt. The increase in the ionic conductivity when more GBL is added to the polymer is a consequence ionic mobility enhancement, provided by transport in a less viscous, "liquid" medium. For a classical polymer electrolyte system (polymer and salt only), a decrease in the ionic conductivity would be expected after a certain salt concentration, due to the formation of ionic pairs and cross-linking points [48,49]. Such effects make the segmental motion of the polymer chains more difficult and, as a consequence, lower the ionic mobility [50]. The addition of GBL to P(EO-EM) allows the dissolution of a higher amount of salt in such a way that the dissolution degree might be comparable to a salt dissolved in an organic solvent.

For all GBL contents, the addition of small amounts of LiI provided a slight increase in the ionic conductivity up to approximately 5 wt.% of this salt. For the polymer electrolyte containing 30 wt.% of GBL, a plateau of $\sim 3 \times 10^{-5}$ S cm^{-1} is observed after this point even with a higher salt content. This plateau is less evident in the samples containing 50 wt.% of GBL and practically disappears at high concentration of the additive. For the samples containing 70 wt.% of GBL, it is interesting to note a sharp increase in the ionic conductivity after 5 wt.% LiI. This behavior will be addressed in the next section using Raman spectroscopy. It was also been observed and discussed by Jerman et al. [51] in a electrolyte containing an ionic liquid and high amount of iodine.

3.2. Raman spectroscopy

Fig. 3 shows the Raman spectra of the gel polymer electrolytes as a function of LiI/I_2 content for the samples containing 30 wt.% (Fig. 3a) and 70 wt.% (Fig. 3b) of GBL. The iodide:iodine molar ratio was kept at 10:1 (wt.%) for all samples. A control sample was prepared only with P(EO-EM)/GBL and no apparent bands in the region of 50–250 cm^{-1} were observed. For the P(EO-EM)/GBL/LiI/I_2 samples, a band observed around 110 cm^{-1} can be assigned to the symmetric stretch of I_3^- species [52,53]. The intensity of this band increases as the concentration of LiI and I_2 in the sample increases. For the samples containing 15 wt.% and 20 wt.% of LiI another band at ~142–145 cm^{-1} can also be observed. This new band is assigned to the vibration mode of higher polyiodide species, such as I_5^-, which have been reported to appear around 145–165 cm^{-1} [51,54]. The band attributed to the molecular vibration of I_2 around 180–210 cm^{-1} was not observed in any of the electrolyte samples, providing additional evidence that all iodine added to the electrolyte was converted into polyiodide species.

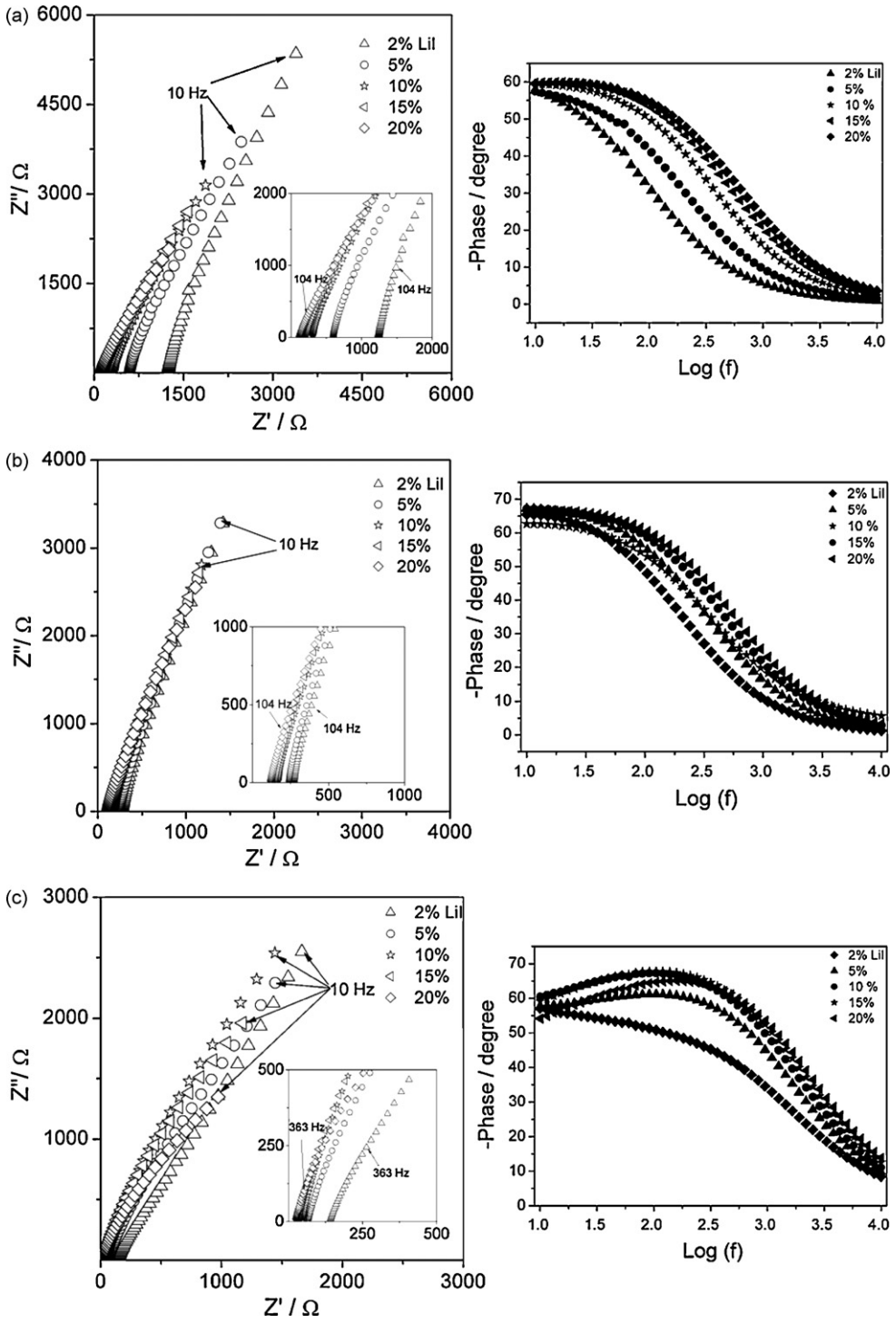

Fig. 1. Nyquist plots and Bode diagram for the gel polymer electrolyte with different salt concentration and GBL content: (a) 30 wt.%, (b) 50 wt.% and (c) 70 wt.% of GBL.

Polyiodides have a lower limiting molar conductivity than monoiodide species due to their larger ionic radius. Thus, considering only the diffusion of ionic species as liable for the conductivity of the electrolytes investigated herein, a decrease in the conductivity values for samples containing larger concentrations of iodide/iodine would be expected. However, it is well known that electron exchange might occur between polyiodides and, under high salt/iodine concentration, the Grothuss-type charge-transfer mechanism might contribute to the effective conductance of the electrolyte [55,56]. In the Grothuss-type charge-transfer mechanism, electron hopping and the polyiodide bond exchange are coupled, contributing to the effective conductance of the polymer electrolyte [54]. Thus, in electrolyte samples where the Grothuss charge-transfer mechanism occurs, we say that the conductor presents both ionic and electronic contributions.

In fact, the results presented in Fig. 2 show that the conductivity values increase at two different rates above 10 wt.% LiI (for the samples containing 50 wt.% and 70 wt.% GBL) and remain constant (for the sample with 30 wt.% GBL), instead of a maximum followed by a decay. This change in the slope of the curves appears at the LiI concentration where the I_5^- species started to form according to

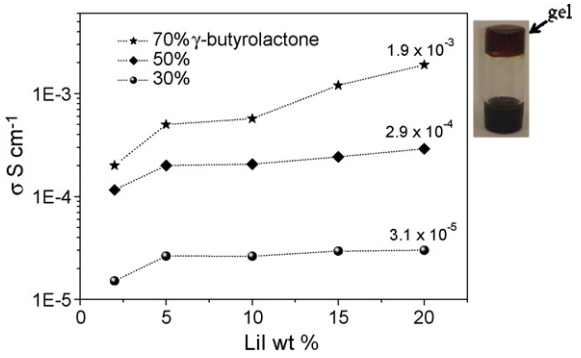

Fig. 2. Ionic conductivity of the gel polymer electrolyte based on poly(ethylene oxide-co-2-(2-methoxyethoxy) ethyl glycidyl ether) (P(EO-EM)) as a function of LiI concentration and GBL content. A picture of the inverted gel electrolyte vessel containing 70 wt.% GBL is also shown.

Raman analysis. This suggests two different types of conductivity mechanisms [51].

Therefore, we can conclude that the gel polymer electrolytes discussed here behave as mixed conductors, presenting both ionic and electronic conductivity above 10 wt.% of LiI, due to the formation of high polyiodide species.

The sharp increase in the conductivity as a function of salt content, observed above 10 wt.% of LiI, is more evident for the electrolyte sample with 70 wt.% GBL (see Fig. 2). This might be due to a faster diffusion dynamics of the iodide/iodine species due to the presence of more GBL. In other words, the medium is much less viscous. More GBL in the system can facilitate the collision of these species in order to generate more high polyiodides. GBL is expected to interact with Li^+, but also with iodine (due to its acceptor character). This effect can be estimated by analyzing the ratio between the polyiodide (I_m^-) and triiodide (I_3^-) species. The I_m^-/I_3^- ratio was calculated from the intensities of the peaks at 110 and 142 cm^{-1}. The ratio was obtained as a function of salt concentration for the gel polymer electrolyte prepared with different GBL content (Fig. 4). We can observe an increase in the I_m^-/I_3^- ratio with the addition of both salt and GBL into the electrolyte. The generation of more polyiodides as the amount of salt/iodine increases was expected and the increase in the I_m^-/I_3^- ratio as a function of GBL content confirms that polyiodide formation benefits from the low viscosity of the medium with more additive.

In summary, the increase in the conductivity observed in Fig. 2 can be identified the appearance of an alternative conduction pathway. In the other words, the polymer electrolytes discussed here present both ionic and electronic contributions, resulting in samples with conductivities that approach liquid electrolytes.

Further investigation needs to be done in order to estimate the contribution of each process (ionic and electronic) to the overall conductivity. Considering the value of the conductivity reached in the present work ($\sim 10^{-3}$ S cm^{-1}), we can infer that in our system, the electronic contribution is small but still significant. The conductivity displayed by our polymer electrolyte is high in comparison to materials presenting only ionic conductivity but it is rather low in comparison to materials that display solely electronic conductivity (metals, for instance).

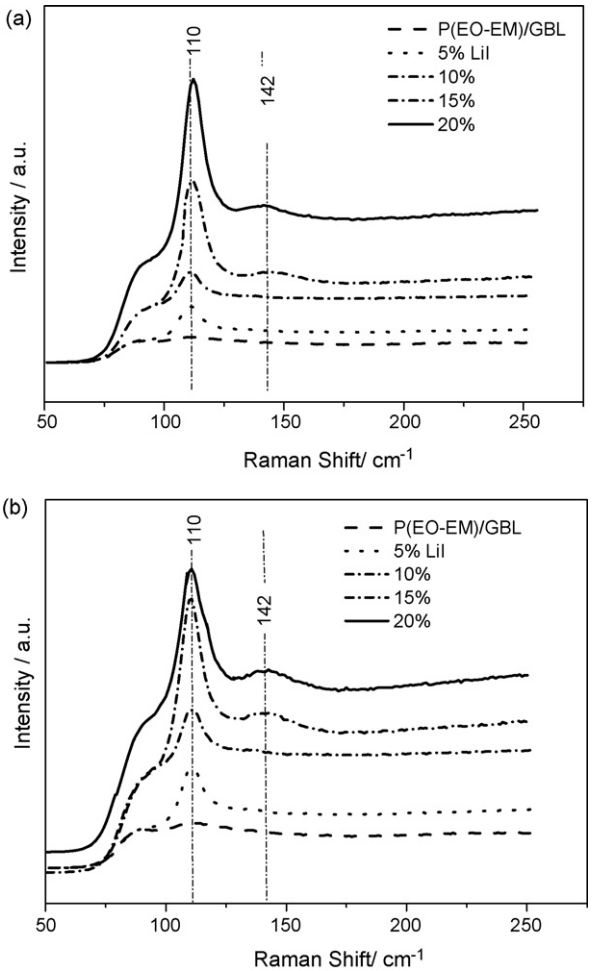

Fig. 3. Raman spectra as a function of LiI concentration for the polymer electrolyte P(EO-EM)/GBL/LiI/I_2 (laser excitation wavelength 632.8 nm). (a) 30 wt.% and (b) 70 wt.% of GBL.

3.3. Thermal analysis

The differential scanning calorimetry (DSC) curves of the pure copolymer, P(EO-EM)/GBL and for all P(EO-EM)/GBL/LiI/I_2 samples with different LiI and GBL concentrations are displayed in Fig. 5. The iodine concentration was calculated for all samples to be 1:10 (wt.%) ratio according to the amount of LiI added.

According to Fig. 4, no crystallinity peaks are observed for the pure copolymer and the sample can be considered fully amorphous, with a low glass transition temperature (T_g) of −66 °C. The increase in the GBL content, in the absence of salt, did not cause any significant change on the T_g value, even when 70 wt.% of the liquid was added. This behavior suggests that GBL is not acting as a plasticizer for the P(EO-EM). In fact, GBL is more likely to be acting as solvent

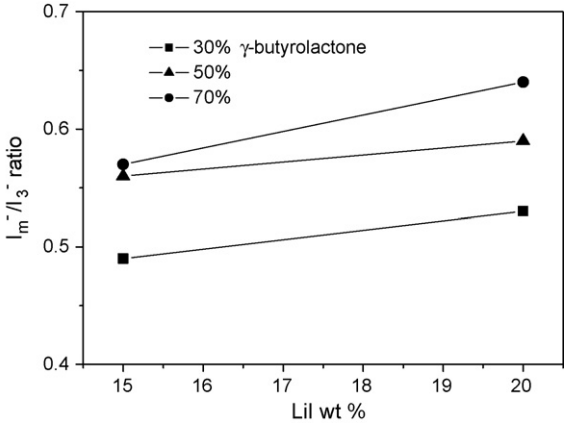

Fig. 4. Ratio of polyiodides (I_m^-) and I_3^- (I_m^-/I_3^-) as a function of salt concentration for the gel polymer electrolyte prepared with different amounts GBL. The iodide:iodine molar ratio was kept at 10:1(wt.%) for all samples.

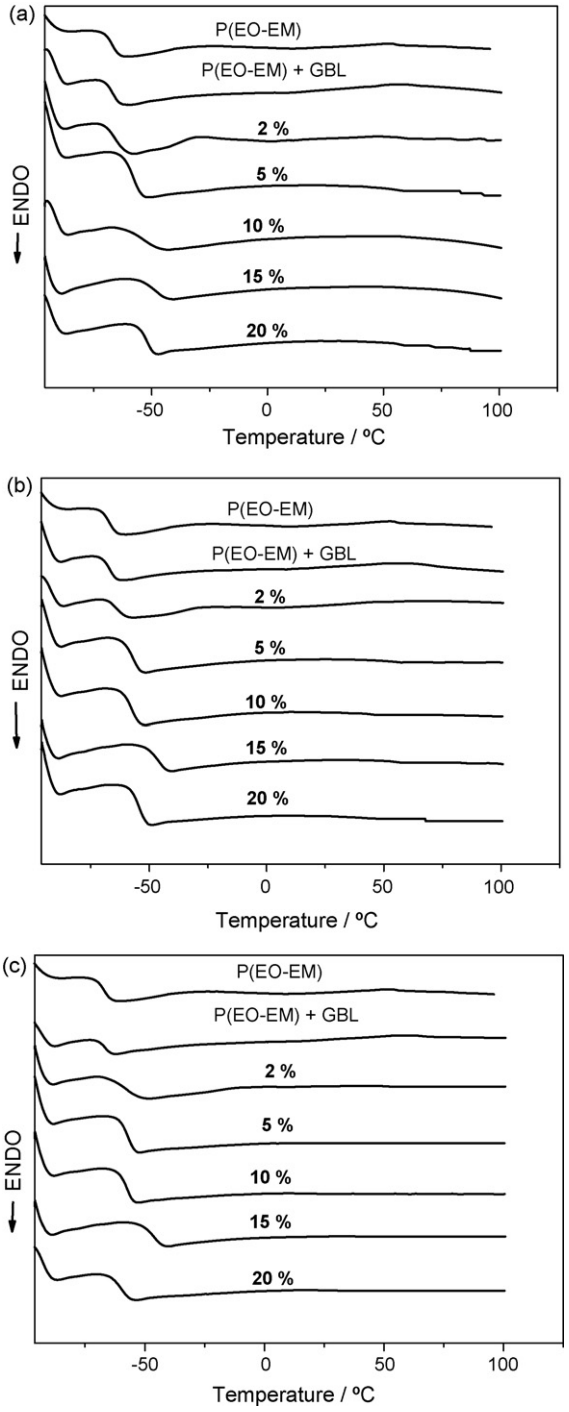

Fig. 5. DSC curves of the P(EO-EM), P(EO-EM)/GBL and gel polymer electrolyte (P(EO-EM)/GBL/LiI/I_2) samples with different salt concentrations: (a) 30 wt.%, (b) 50 wt.% and (c) 70 wt.% of GBL.

for both salt and polymer and we expect that, at ambient conditions, P(EO-EM), GBL and LiI are all mixed. Table 1 summaries the T_g values obtained from the DSC data.

As observed in Table 1, the T_g values of the polymer increases as the LiI concentration increases for all the GBL contents. The increase in the T_g values is expected in the presence of salt. This is a consequence of the formation of reticulation points from the strong ion–dipole interaction between the polymer heteroatoms and Li^+ ions, lowering polymer chain mobility [50]. This behavior has already been observed in polymer electrolytes composed of poly(ethylene oxide) and its copolymers with lithium salts

Table 1
Glass transition temperatures (T_g) from the DSC curves for the pure copolymer containing GBL and for the gel polymer electrolytes with different concentrations of GBL and salt.

LiI content (wt.%)	30 wt.% GBL	50 wt.% GBL	70 wt.% GBL
0	−66 °C	−66 °C	−66 °C
2	−64 °C	−63 °C	−63 °C
5	−58 °C	−56 °C	−56 °C
10	−54 °C	−57 °C	−57 °C
15	−49 °C	−46 °C	−48 °C
20	−48 °C	−52 °C	−59 °C

[48,50]. An exception, however, occurred for the samples containing 30 wt.%, 50 wt.% and 70 wt.% GBL, where a drop in the T_g value has occurred. Apparently, with these conditions of high amounts of salt and additive, it seems that these components are interacting strongly, diminishing the interaction with the polymer chains.

3.4. DSSC characterization

The *J–V* curves of the DSSCs based on TiO_2 porous nanostructured electrodes (under 10 and 100 mW cm^{-2} conditions) employing the gel polymer electrolyte P(EO-EM)/LiI/I_2 with several different GBL contents are shown in Fig. 6. The photocurrent density (J_{sc}), open-circuit voltage (V_{oc}), fill factor (FF) and the corresponding energy conversion efficiency (η) values, are summarized in Table 2. The series resistance of the system (R_s) and the fitting constants (m_1 and m_2) values obtained after fitting the curves using a two diode model are also included [34,36,57]. The *J–V* curves do not fit using a one diode model because of a high rate of charge recombi-

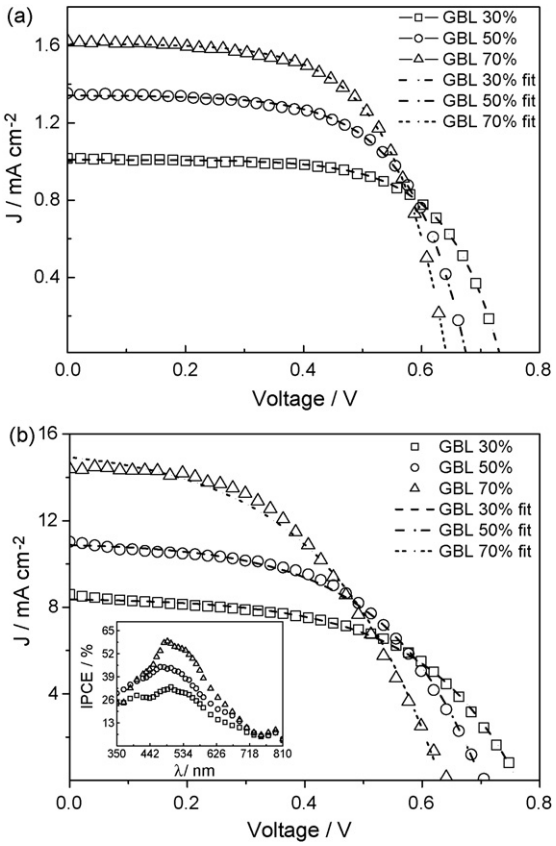

Fig. 6. *J–V* curves of the DSSCs assembled with the gel polymer electrolytes at different GBL contents and fixed salt concentration (20 wt.%). (a) 10 mW cm^{-2} and (b) 100 mW cm^{-2}. Active cell area: 0.25 cm^2. The dashed lines represent the fitting curves according to a two diode equation [36]. The insert in (b) shows the incident photon-to-current conversion efficiency (IPCE) spectra.

Table 2
J–V electrical parameters of the dye-sensitized solar cells with gel polymer electrolyte (P(EO-EM)/GBL/LiI/I_2) containing different GBL content at a fixed salt concentration (20 wt.%) under 100 and 10 mW cm^{-2} illumination.

	V_{oc} (V)	J_{sc} (mA cm^{-2})	FF	η (%)	m_1	m_2	R_s Ω
10 mW cm^{-2}							
70 wt.% GBL	0.63	1.63	0.62	6.5	3.8	3.6	52
50 wt.% GBL	0.67	1.35	0.63	5.7	3.7	3.5	75
30 wt.% GBL	0.73	1.01	0.65	4.9	4.3	3.5	80
100 mW cm^{-2}							
70 wt.% GBL	0.64	14.5	0.47	4.4	3.8	7.4	52
50 wt.% GBL	0.70	11.0	0.53	4.0	3.7	6.1	75
30 wt.% GBL	0.76	8.5	0.53	3.4	4.3	6.6	80

nation in devices using polymeric or gel electrolyte. Thus, in order to fit the *J–V* curves a second term must be added, introducing a contribution from a light dependent recombination current.

Recently, we reported that the concentration of 20 wt.% LiI is preferable because high salt (and iodine) concentrations also contribute to increase the dark current and the additional contribution to the photocurrent is minimal [34]. Thus, all devices presented here have an electrolyte containing 20 wt.% LiI (and 2 wt.% I_2).

The increase in the conductivity of the gel polymer electrolyte as more GBL is present directly influences the photocurrent values at both illuminations. This is a consequence of an increase in the mobility of the redox species in the polymer electrolyte, intensifying the mass transport in such medium.

The inset in Fig. 6b shows the incident photon-to-current conversion efficiency as a function of the wavelength (IPCE) of the solar cells based on P(EO-EM)/GBL/LiI/I_2. The IPCE curves resemble the absorption spectrum of the N-719 dye with a maximum peak at ~530 nm. Since the conductivity of the gel polymer electrolyte is one of the major photocurrent limiting factors in a DSSC, its influence can be observed in the IPCE spectra, where the device assembled with the gel electrolyte containing 70 wt.% GBL gives rise to an IPCE value close to 60%.

Nonetheless, the V_{oc} values displayed an opposite trend, as observed for the photocurrent values. The factors that influence this behavior will be carefully discussed in the next section.

Since the energy conversion efficiency (η) is proportional to both V_{oc} and J_{sc} values, the high J_{sc} values observed in this work compensate the loss in V_{oc} when the amount of GBL increases in the gel polymer electrolyte. Thus, the electrolyte containing 70 wt.% of additive gives rise to the best efficiency, with η equal to 4.4% at 100 mW cm^{-2}. It is important to indicate that this is an expressive value considering the nature of the electrolyte. Even reaching conductivity values close to 1 mS cm^{-1} the photocurrent is still expected to be limited by the diffusion of the triiodide (and higher polyiodide) species in the electrolyte and an increase in the overall energy conversion must include simultaneous optimization of other important parameters such as electrolyte penetration, charge transfer at the interfaces and minimization of the dark current [58]. It is also interesting to note that the value 1 mS cm^{-1} obtained by our gel polymer electrolyte (close to liquid systems) does not correspond to the J_{sc} values obtained in DSSCs using liquid electrolyte. This is because such conductivity was reached after the formation of the polyiodide species and, as a consequence, after the introduction of an electronic pathway. However, this has not contributed to accelerate iodide diffusion; in other words, the electronic pathway makes the electrons move faster from one electrode to other but does not do the same with the iodide ions, which are essential for cation regeneration.

At low light intensity a new balance was established between J_{sc} and V_{oc} values and the solar cells with low additive content (30 wt.%) exhibit the highest overall conversion efficiency (5.7%). This can be a consequence of a modest variation in the photocurrent density compared to the change in the V_{oc} values. In other words, at low light intensity, fewer electrons are photogenerated and the demand for a highly conductive medium to compensate for dye cation regeneration is not crucial [20].

The low FF values reflect the high series resistance (Table 2) of all DSSCs studied herein. These resistance losses arise from the lower ionic mobility of the redox species, thickness of the TiO_2 film are resistances of the FTO glass and contacts. As observed in Table 2, the series resistance values (R_s) are correlated with the conductivity data, where the samples with high conductivity exhibit lower R_s values. The m_1 and m_2 values are related to charge recombination and to the light dependent recombination current, respectively. As m_1 values were determined first by fitting the dark *J–V* data, they appear to not change at different illuminations; however, the m_2 values double at 100 mW cm^{-2}, suggesting that in fact such recombination is important to device's performance.

As indicate in Fig. 6, the V_{oc} values decrease as the amount of additive increased in the polymer. In DSSC, a decrease in the voltage can come about because of a decrease in the band offset (TiO_2 conduction band relative to iodine/iodide potential) or because of an increased recombination rate constant (photoinjected electrons with dye cation and/or triodide species in the electrolyte). Thus, photovoltage decay measurements and transient absorption spectroscopy data were carried out in order to help the discussion of such puzzling behavior.

First, we shall address the effect of small cations and/or protons in the band offset of the TiO_2 film. It is well established that small cations and protons intercalate in the TiO_2, structure leveling off the flatband potential of the polycrystalline semiconductor [59,60].

In our system, acid–base interactions between the Li^+ ions with the ethylene oxide units of the polymer chains and the additive (in our case, gamma-butyrolactone) can occur. Both polymer and GBL can coordinate lithium ions. It is expected that the coordination by the polymer chain is more effective, leading to a strong ion–dipole interaction [16]. Thus, by increasing the amount of GBL, we could suppose that more lithium ions are expected to be "free" and intercalated or adsorbed in the nanoporous TiO_2 structure. Besides, our polymer has a molar mass of $\sim 1 \times 10^6$ g mol^{-1} so that, even using a vacuum procedure to deposit it in the TiO_2 film, a completed penetration into the inner pores may be difficult to obtain. The opposite, however, is not expected for Li^+ coordinated to the small GBL molecules. Although an increase in the local concentration of Li^+ cations in the TiO_2 film may be responsible for a shift in the Fermi level, we do not believe that this is the case. GBL is also a coordinating molecule and such variation in the Li^+ concentration from one composition to another could not explain by itself the decreases in the V_{oc} of more than 0.1 V, although a minor influence on the effect observed in the V_{oc} cannot be neglected. TAS demonstrated that acceleration in the charge recombination due to an increase in the occupancy of the conduction/trap states influenced by an increase of Li^+ concentration has, in fact, occurred. However, as it will be shown later, this acceleration was minimal and other factors may predominate.

Turning to the effect of charge recombination on the photovoltage, two recombination pathways exist at the interface between the sensitized metal-oxide and the redox active electrolyte. One is the re-reduction of the dye cation by photoinjected electrons (Eq. (1)) and the other is the recombination of photoinjected electrons directly with oxidized species in the electrolyte (also called back reaction). In the commonly used iodine/iodide redox couple, this second recombination reaction is expressed by Eq. (2).

$$Dye^+ + e^-(TiO_2) \rightarrow Dye \quad (1)$$

$$2e^-(TiO_2) + I_3^- \rightarrow 3I^- \quad (2)$$

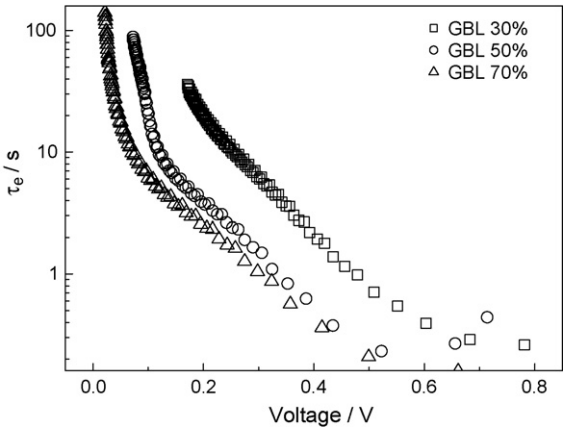

Fig. 7. Behavior of the electron lifetime (τ_e) from the DSSCs based on polymer gel electrolyte with different GBL contents at a fixed salt concentration (20 wt.%) for all samples. The τ_e values were estimated from Eq. (3) [38].

In DSSC assembled with a liquid electrolyte, rapid regeneration of dye cation by the iodide ions compete effectively with the charge recombination expressed by Eq. (1), and, as a consequence, the charge recombination with the electrolyte (triiodide species) is the primary recombination loss pathway limiting these devices [61]. In DSSC assembled with a classical polymer electrolyte however, the slow diffusion of the iodide ions and the accumulation of I_3^- species in the vicinity of the TiO_2/dye film make the two recombination pathways coexist, limiting the device's efficiency [36].

The electron lifetime (τ_e) can be estimated from the voltage decay transients according to Eq. (3) [38]:

$$\tau_e = -\frac{kT}{e}\left(\frac{dV_{oc}}{dt}\right)^{-1} \quad (3)$$

The behavior of the electron lifetime of the DSSC assembled in this work under open-circuit conditions is shown in Fig. 7.

The exponential-like increase in the electron lifetime as the voltage decreases under open-circuit conditions is in excellent agreement to the results reported by Quintana et al. [37]. The electron lifetime decreases as more GBL is added to the polymer, corroborating the trend in V_{oc} values observed in Fig. 6. These results support the observation of an increase in the charge recombination at the TiO_2/dye electrolyte interface as the amount of polymer is decreased in the electrolyte.

As all electrolyte samples were initially prepared with the same amount of I_2 and LiI, we expect that the overall amount of polyiodide species remains unchanged and that any decrease in the photovoltage due to an increase in the amount of the iodine can be ruled out [54].

According to Fig. 4, a change has occurred in the proportion between the I_5^-/I_3^- ratio and the sample with high amounts of GBL is the one with higher proportion of I_5^- in the electrolyte. Two possible explanations can be proposed based on the different ratios between these two polyiodide species. Because of the size of the I_5^- ion, the charge is more delocalized and electron repulsion must be less pronounced, favoring a faster recombination. Besides, I_5^- also exhibits a lower diffusion in comparison to the I_3^- ion due to its size and a buildup of such species close to the TiO_2 surface must be relevant.

Theoretical calculations are described in Table 3 for the two basis sets used in this work and they show that the pentaiodide is a better electron acceptor than the triiodide since the electron affinity (*EA*) for that species is greater. Absolute energies for the lowest unoccupied molecular orbital (LUMO) cannot be used to obtain exact electron affinities, but the same conclusions can be obtained when their energies are compared: the orbital energy for the pentaiodide is lower for both basis sets.

Table 3
Electron affinities and LUMO energies for the polyiodide anions in eV.

Species	SV4(2d)		ANODZP	
	LUMO	*EA*	LUMO	*EA*
I_3^-	0.64	−2.38	0.68	−2.58
I_5^-	−0.96	−0.43	−0.99	−0.48

It seems that charge recombination with electrolyte is indeed the major contributing factor to the observed values of photovoltage. Although recombination with dye cation is discarded in DSSC using liquid electrolyte, we have proved that it is relevant in devices using classical polymer electrolyte (polymer and salt only) [36]. Can we discard its influence in solar cells using a gel polymer electrolyte? An elegant way to analyze the kinetics of recombination and regeneration is the evaluation of transient absorption studies (TAS).

More recently, using TAS we also addressed such competition studying DSSC assembled with gel polymer electrolyte with different LiI concentrations [34]. Acceleration in dye cation regeneration was observed when the amount of LiI was increased in the electrolyte and apparently such competition is minimized with high availabilities of iodide ions [34]. Here, TAS measurements were carried out in order to study such competition when different amounts of GBL are added to the system.

Transient decays were obtained for TiO_2/dye films using an inert electrolyte containing 20 wt.% of $LiClO_4$. The difference was in the amount of GBL, 30 wt.% and 70 wt.%. Using such electrolytes, the decay of the transient signal, attributed to dye cation absorption, is purely due to the recombination between electrons and the dye cations. The half time were estimated to be 30 μs and 10 μs for the electrolyte containing 30 wt.% and 70 wt.% of GBL, respectively (data not shown). For the electrolyte composed of polymer and NaI/I_2 (without any additive) we reported a half-time of 2 ms [36]. In our work, the acceleration observed in dye cation decay when the liquid additive is present in the polymer can be related to an increase in the occupancy of the conduction/trap states, induced by the presence of more "free" lithium ions in the electrolyte [62]. However, such accelerations were negligible when we increased the GBL content from 30 wt.% to 70 wt.% (30–10 μs) if compared to the sample without additive (2 ms). These results indicated that this charge recombination maybe be relevant in conditions where the regeneration reaction is not effective.

Fig. 8 shows the transient absorption data of the TiO_2/dye films in the presence of the gel polymer electrolyte P(EO-EM)/GBL/LiI/I_2. In this experiment the decays of the cation absorption band, at 810 nm, under open-circuit and dark conditions were monitored. The amount of GBL added in these systems was 30 wt.% and 70 wt.%. The concentration of LiI and I_2 was fixed in 20 wt.% and 2 wt.% for all samples.

In the presence of I^- ions, the decay of the photoinduced absorption at 810 nm is biphasic. The fast phase (1–100 μs) is assigned to decay of the dye cation, whereas the slow phase is assigned to decay of I_2^- species generated according to the reaction shown in Eq. (4) [36,62]:

$$Dye^+ + 2I^- \rightarrow Dye + I_2^- \quad (4)$$

At first analysis, no difference could be observed in the fast phase and the half-time of the dye cation decay was estimated to be ~1 μs. The decay of the dye cation can result from both re-reduction by iodide ions and/or by charge recombination with injected electrons. The observation of a significant yield of I_2^- strongly indicates that the former occurs with a high yield.

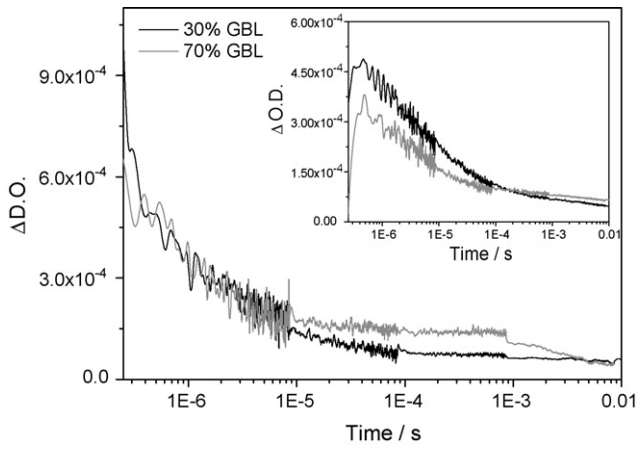

Fig. 8. Transient absorption spectra (TAS) for dye-sensitized TiO_2/dye films covered with gel polymer electrolyte containing 30 wt.% (black) and 70 wt.% (gray) of GBL. The concentrations of LiI and I_2 were fixed at 20 wt.% and 2 wt.%, respectively, for all samples. The inset corresponds to the dye cation decay dynamics for the same device assembled with the gel electrolyte containing a reduced LiI concentration (7 wt.% of LiI and 13 wt.% of $LiClO_4$).

The amplitude of the slower phase increases as the amount of GBL increases, an indication of a high yield of I_2^- in the electrolyte sample containing more liquid additive. This is a consequence of the higher mobility of the iodide ions when the medium is less viscous. In other words, although the amount of LiI is the same in both cases, the diffusion is faster in the electrolyte with more GBL, making the regeneration reaction faster for this sample.

The effectiveness of the system with more GBL in the regeneration reaction can be seen in the inset of Fig. 8. The inset exhibits the transient decay for the samples containing 7 wt.% of LiI and 13 wt.% of $LiClO_4$ (in order to keep the same concentration of Li^+ ions) and 30 wt.% or 70 wt.% GBL. In a condition where the concentration of iodide is low, the electrolyte containing 70 wt.% of GBL displays a faster decay, as expected due to the increase in the ionic mobility of the iodide ions in this electrolyte. The half-times of the dye cation decay was ~5 and 2.5 μs for the electrolyte containing 30 wt.% and 70 wt.% of GBL, respectively.

The TAS data presented here shows that the addition of GBL has accelerated both dye cation regeneration by the iodide ions and pure charge recombination (electrons from the TiO_2 conduction band/trap states with dye cations). Indeed, the regeneration reaction is marginally faster than the recombination reaction (2.5 *versus* 10 μs). These results indicate that when the electrolyte is composed solely of polymer and salt, charge recombination competes with regeneration because the latter is slow; however, in the gel electrolyte, although regeneration becomes faster, they compete with each other because charge recombination is also accelerated (from a ms to a μs time scale).

The acceleration observed in "pure" charge recombination; however, does not explain the decrease in the photovoltage of more than 0.1 V since the difference in the rate of the kinetics for the samples containing 30 wt.% and 70 wt.% GBL is minimal (10 *versus* 30 μs). We can conclude that the decrease in the photovoltage as the amount of liquid component is added is more strongly influenced by the "back reaction" (recombination with the electrolyte). However, the other two contributions (shift in the flat band potential due to more Li^+ intercalation and acceleration of the "pure" charge recombination) also influence this behavior and cannot be ignored.

4. Conclusions

The addition of γ-butyrolactone in the polymer electrolyte based on poly(ethylene oxide-co-2-(2-methoxyethoxy)ethyl glycidylether)/LiI/I_2 improved the ionic conductivity by two orders of magnitude, being responsible for the increase in the photocurrent values of the DSSC. However, even after addition of 70 wt.% of liquid component the I_{SC} is still limited by the diffusion of the triodide species. Above 10 wt.% LiI, for all samples with different GBL content, we observed a change in the transport mechanism. In fact, above this salt concentration, the formation of higher polyiodide species, such as I_5^- was confirmed by Raman spectroscopy. In these conditions the gel electrolyte can be considered as a mixed conductor, where electronic and ionic transport coexist, leading to conductivity values of $\sim 10^{-3}$ S cm^{-1}.

More additive in the polymer has also changed the I_m^-/I_3^- ratio and this has an important influence on the charge recombination dynamics at the TiO_2/dye–eletrolyte interface.

TAS studies indicated that, with addition of GBL in the electrolyte, dye cation regeneration also becomes faster and this is evidence of a faster transport of the iodide ions in the electrolyte, corroborating the conductivity data.

The decrease in the V_{oc} values observed when more GBL is added to the polymer is a more complex issue. Photovoltage decay measurements confirm that recombination is higher in the less viscous electrolyte. Although the recombination with the electrolyte is expected to dominate, we cannot discard that the increase of the local Li^+ concentration in the TiO_2 film as GBL content increases can also be important. More Li^+ ions increase the occupancy of the conduction/trap states and a downward shift in the band offset can be obtained. In fact, TAS studies reveal that the addition of a liquid component makes the charge recombination with dye cations faster (from milliseconds for the electrolyte without additive to microseconds when GBL is present). However, once the liquid component is present, these variations are not relevant (from 30 μs to 10 μs). It is also important to point out that this time scale is marginally faster than dye cation regeneration (~1 μs) and a competition between "pure" charge recombination and regeneration cannot be discarded in our system.

Although several factors might be contributing to decrease the photovoltage, we conclude that it is the recombination with the electrolyte that is the most important pathway determining the photovoltage. The increase in the I_5^-/I_3^- ratio as more GBL is present seems to accelerate this recombination. Higher polyiodides are expect to diffuse less from one electrode to another and can accumulate in the TiO_2/dye interface. In addition, their more delocalized charge makes the reaction with electrons more favorable due to less electron repulsion. In fact, theoretical calculations showed that I_5^- possesses a higher electron affinity.

Along the years the search for more conductive media without loosing their "solid nature" was the dream of researchers working in the field of polymer and gel electrolytes applied to DSSC. We have demonstrated here that the achievement of electrolytes with high conductivity does not *per se* guarantee solar cells with efficiency comparable to devices with liquid electrolytes. Even through attaining "solid" electrolytes with high conductivity, this study showed that recombination at the interface is the major influence in the device's efficiency, limiting the photovoltage values. And, in order to obtain solar cells with better performance, not only the electrolyte needs to be modified but also the interface deserves more attention. Core-shell electrodes, blocking electrodes, nanotubes or nanorods structures are alternatives that, together with an electrolyte engineering, can result in more efficient "solid-state" DSSCs.

Acknowledgements

The authors acknowledge FAPESP (fellowships 06/58998-3 and 08/51001-9), CNPq and Renami for financial support, Daiso Co., Ltd. (Osaka, Japan) for kindly providing the copolymer and Prof. Carol H. Collins for the English revision. We also acknowledge Prof. Victor Baranauskas (Electrical Engineer/UNICAMP) for the Raman facility and the LMF/LNLS (National Synchrotron Light Laboratory, Campinas, SP, Brazil) for technical support.

References

[1] B. O'Regan, M. Grätzel, Nature 353 (1991) 737.
[2] M. Grätzel, Actual. Chim. 308 (2007) 57.
[3] P. Wang, S.M. Zakeeruddin, J.E. Moser, R.H. Baker, M. Grätzel, J. Am. Chem. Soc. 126 (2004) 7124.
[4] S. Ito, S.M. Zakeeruddin, P. Comte, P. Liska, D. Kuang, M. Grätzel, Nat. Photonics 2 (2008) 693.
[5] J. Bandara, H. Weerasinghe, Sol. Energy Mater. Sol. Cells 85 (2005) 385.
[6] G.K.R. Senadeera, T. Kitamura, Y. Wada, S. Yanagida, J. Photochem. Photobiol. A Chem. 184 (2006) 234.
[7] J.E. Kroeze, N. Hirata, L. Schmidt-Mende, C. Orizu, S.D. Ogier, K. Carr, M. Gratzel, J.R. Durrant, Adv. Funct. Mater. 16 (2006) 1832.
[8] T. Kato, A. Okazaki, S. Hayase, J. Photochem. Photobiol. A Chem. 179 (2006) 42.
[9] J.N. Freitas, C. Longo, A.F. Nogueira, M.-A. De Paoli, Sol. Energy Mater. Sol. Cells 92 (2008) 1110.
[10] J. Wu, Z. Lan, J. Lin, M. Huang, S. Hao, T. Sato, S. Yin, Adv. Mater. 19 (2007) 4006.
[11] J.N. Freitas, A.F. Nogueira, M.-A. De Paoli, J. Mater. Chem. 19 (2009) 1, doi:10.1039/b900928k.
[12] B.I. Ito, J.N. Freitas, M.-A. De Paoli, A.F. Nogueira, J. Braz. Chem. Soc. 19 (2008) 688.
[13] C.A. Vincent, Solid State Chem. 17 (1987) 167.
[14] C.P. Fonseca, S. Neves, J. Power Sources 104 (2002) 85.
[15] S.S. Sekhon, N. Arora, H.P. Singh, Solid State Ionics 160 (2003) 301.
[16] F.M. Gray, Solid Polymer Electrolytes, Fundamentals and Technological Applications, VCH Publishers, New York, 1991.
[17] E. Tuchida, H. Ohno, K. Tsunemi, N. Kobayashi, Solid State Ionics 11 (1983) 227.
[18] T. Stergiopoulos, I.M. Arabatzis, G. Katsaros, P. Falaras, Nano. Lett. 2 (2002) 1259.
[19] G. Katsaros, T. Stergiopoulos, I.M. Arabatzis, K.G. Papadokostaki, P. Falaras, J. Photochem. Photobiol. A Chem. 149 (2002) 191.
[20] V.C. Nogueira, C. Longo, A.F. Nogueira, M.A. Soto-Oviedo, M.A. De Paoli, J. Photochem. Photobiol. A Chem. 181 (2006) 226.
[21] A.F. Nogueira, J.R. Durrant, M.A. Paoli, Adv. Mater. 13 (2001) 826.
[22] S. Nakade, T. Kanzaki, Y. Wada, S. Yanagida, Langmuir 21 (2005) 10803.
[23] T. Kato, A. Okazaki, S. Hayase, Chem. Commun. (2005) 363.
[24] J.E. Benedetti, M.A. De Paoli, A.F. Nogueira, Chem. Commun. (2008) 1121.
[25] H. Usui, H. Matsui, N. Tanabe, S. Yanagida, J. Photochem. Photobiol. A Chem. 164 (2004) 97.
[26] T. Kato, T. Kado, S. Tanaka, A. Okazaki, S. Hayase, J. Electrochem. Soc. 153 (2006) A626.
[27] T. Kato, S. Hayase, J. Electrochem. Soc. 154 (2007) B117.
[28] Y.J. Kim, J.H. Kim, M.S. Kang, M.J. Lee, J. Won, J.C. Lee, Y.S. Kang, Adv. Mater. 16 (2004) 1753.
[29] M.S. Kang, J.H. Kim, Y.J. Kim, J. Won, N.G. Park, Y.S. Kang, Chem. Commun. (2005) 889.
[30] W. Kubo, T. Kitamura, K. Hanabusa, Y. Wada, S. Yanagida, Chem. Commun. (2002) 374.
[31] S. Sakaguchi, H. Ueki, T. Kato, T. Kado, R. Shiratuchi, W. Takashima, K. Kaneto, S. Hayase, J. Photochem. Photobiol. A Chem. 164 (2004) 117.
[32] T. Kato, M. Fujimoto, T. Kado, S. Sakaguchi, D. Kosugi, R. Shiratuchi, W. Takashima, K. Kaneto, S. Hayase, J. Electrochem. Soc. 152 (2005) A1105.
[33] S. Mikoshiba, S. Murai, H. Sumino, S. Hayase, Chem. Lett. (2002) 918.
[34] J.N. Freitas, A.S. Gonçalves, M.A. De Paoli, J.R. Durrant, A.F. Nogueira, Electrochim. Acta 53 (2008) 7166.
[35] H.W. Han, U. Bach, Y.B. Cheng, R.A. Caruso, Appl. Phys. Lett. 90 (2007) 213510.
[36] A.F. Nogueira, M.A. De Paoli, I. Montanari, R. Monkhouse, J. Nelson, J.R. Durrant, J. Phys. Chem. B 105 (2001) 75174.
[37] M. Quintana, T. Edvinsson, A. Hagfeldt, G. Boschloo, J. Phys. Chem. B 111 (2007) 1035.
[38] A. Zaban, M. Greenshtein, J. Bisquert, Chem. Phys. Chem. 4 (2003) 859.
[39] J.N. Clifford, E. Palomares, Md.K. Nazeeruddin, M. Grätzel, J.R. Durrant, J. Phys. Chem. C 111 (2007) 6561.
[40] S.B. Sharp, G.I. Gellene, J. Phys. Chem. A 101 (1997) 2192.
[41] A.D. Becke, J. Chem. Phys. 98 (1993) 5648.
[42] J. Andzelm, M. Klobukowski, E. Radzio-Andzelm, J. Comput. Chem. 5 (1984) 146.
[43] B.O. Roos, R. Lindh, P.-A. Malmqvist, V. Veryazov, P.-O. Widmark, J. Phys. Chem. A 108 (2004) 2851.
[44] J.R. MacCallum, C.A. Vincent (Eds.), Polymer Electrolyte Reviews—1 and 2, Elsevier, Essex, England, 1989.
[45] S. Rajendran, M. Sivakumar, R. Subadevi, Solid State Ionics 167 (2004) 335.
[46] S. Rajendran, M. Sivakumar, R. Subadevi, Mater. Lett. 58 (2004) 641.
[47] K. Perera, M.A.K.L. Dissanayake, P.W.S.K. Bandaranayake, Mater. Res. Bull. 39 (2004) 1745.
[48] A.F. Nogueira, M.A.S. Spinacé, W.A. Gazotti, E.M. Girotto, M.A. De Paoli, Solid State Ionics 140 (2001) 327.
[49] A.F. Nogueira, M.A. De Paoli, Sol. Energy Mater. Sol. Cells 61 (2000) 135.
[50] G.G. Silva, N.H.T. Lemes, C.N.P. Fonseca, M.A. De Paoli, Solid State Ionics 93 (1996) 105.
[51] I. Jerman, V. Jovanovski, A.S. Vuk, S.B. Hocevar, M. Gaberscek, A. Jesih, B. Orel, Electrochim. Acta 53 (2008) 2281.
[52] L. Andrews, E.S. Prochaska, A. Loewenschuss, Inorg. Chem. 19 (1980) 463.
[53] M.A. Tadayyoni, P. Gao, M.J. Weaver, J. Electroanal. Chem. 198 (1986) 125.
[54] W. Kubo, K. Murakoshi, K. Kitamura, S. Yoshida, M. Haruki, H. Hanabusa, H. Shirai, Y. Wada, S. Yanagida, J. Phys. Chem. B 105 (2001) 12809.
[55] N. Papageorgiou, T. Athanassov, M. Armand, P. Bonhôte, H. Pettersson, A. Azam, M. Grätzel, J. Electrochem. Soc. 143 (1996) 3099.
[56] G.P. Kalaignan, M.S. Kang, Y.S. Kang, Solid State Ionics 177 (2006) 1091.
[57] C.O. Avellaneda, A.D. Goncalves, J.E. Benedetti, A.F. Nogueira, Electrochim. Acta (2009), doi:10.1016/j.electacta.2009.05.024.
[58] M.S. Kang, J.H. Kim, J. Won, Y.S. Kang, J. Phys. Chem. C 111 (2007) 5222.
[59] D.J. Fitzmaurice, M. Eschle, H. Frei, J.E. Moser, J. Phys. Chem. 97 (1993) 3806.
[60] Y. Liu, A. Hagfeldt, X.R. Xiao, S.E. Lindquist, Sol. Energy Mater. Sol. Cells 55 (1998) 267.
[61] I. Montanari, J. Nelson, J.R. Durrant, J. Phys. Chem. B 106 (2002) 12203.
[62] S.A. Haque, Y. Tachibana, R. Willis, J.E. Moser, M. Grätzel, D.R. Klug, J.R. Durrant, J. Phys. Chem. B 104 (2000) 538.